Vietnam Journal of Mechanics, VAST, Vol. 43, No. 3 (2021), pp. 253 – 264
DOI: https://doi.org/10.15625/0866-7136/15764

EXPERIMENTAL AND NUMERICAL EVALUATION OF THERMODYNAMIC EFFECT ON NACA0015 HYDROFOIL CAVITATION IN HOT WATER

Anh Dinh Le[1,*]
[1]*School of Aerospace Engineering, VNU-University of Engineering and Technology, 144 Xuan Thuy street, Cau Giay district, Hanoi, Vietnam*
[*]E-mail: anh.ld@vnu.edu.vn

Received: 17 December 2020 / Published online: 04 August 2021

Abstract. In this study, the cavitation in hot water, which implies tight interaction of thermodynamic effect, phase change phenomena, and flow behavior, was studied by a combination of experiment and numerical simulation. The experiment in water up to 90°C was performed in the high temperature and high-pressure water tunnel with NACA0015 as a cavitator. The temperature inside the cavity was measured using the high-accuracy thermistor probe. According to the result, the temperature depression in the cavity was increased proportionally with the increase of freestream temperature. The inverse thermodynamic effect was observed with the increase of cavity length when temperature increased. The maximum temperature depression of about 0.41°C was measured in the water at around 90°C. The temperature drop was reasonably captured in simulation by coupling our simplified thermodynamic model with our cavitation model and governing equations. The tendency of temperature depression in the cavity agreed well with experimental data under different flow conditions.

Keywords: cavitation, computational fluid dynamics, thermodynamic, NACA0015.

1. INTRODUCTION

The thermodynamic effect, which easily appears in cryogenic or hot water, is known as the good effect for the hydraulic machine. When cavitation occurs, the latent heat for vaporization is absorbed from the surrounding liquid, thus surrounding liquid temperature is decreased. Since cavitation is mainly governed by saturated vapor pressure, which is proportionality to fluid temperature, evaporation is hard to occur. Thus, the cavitation is suppressed. Hence, to improve the performance of hydraulic machines, the effective use of the thermodynamic effect should be considered and should be clarified in the design of the hydraulic machine. Moreover, for fluids such as cryogenic liquids or hot water, the cavitation implies the complex interaction between thermodynamic effect, phase change, and flow behavior such as turbulence.

The cavitation experiment in water at 95°C was performed in a venturi nozzle by Petkovsel et al. [1,2]. The temperature distribution along the nozzle was measured using a high-speed IR thermography with the maximum temperature depression was of about 0.4°C. Yamaguchi et al. conducted the cavitation experiment on NACA0015 hydrofoil in water with wide range temperature [3]. The temperature depression was measured using the thermistor probes, in that the maximum temperature depression of 0.3°C was observed on the supercavitation condition at 80°C. These experiments indicate that the thermodynamic effect, which is normally negligible in water at room temperature, is visible in hot water cavitation. On the other hand, Cervone et al. conducted the cavitation experiment on NACA0015 hydrofoil in water up to 70°C [4]. The inverse thermodynamic effect was visualized in their experiment, where cavitation became longer and thicker when the freestream temperature increases. It shows that the thermodynamic effect on cavitation has not yet been clarified.

Regarding Computational fluid dynamics (CFD), a homogeneous model is a powerful tool for the numerical simulation of cavitation. Several numerical studies of the thermodynamic effect on cavitation based on a homogeneous model have been conducted using two different approaches. 1) the indirect method, in that the saturated vapor pressure drop is modified without solving an energy conservation equation, and 2) the direct method, where the saturated vapor pressure is calculated based on the temperature field by solving an energy conservation equation. The first approach was proposed by Tsuda et al. [5], and was applied to different objects in cryogenic liquids or refrigerants. The latter approach was proposed by Hosangadi et al. [6]. They conducted the simulation of cavitation in liquid nitrogen and liquid hydrogen on a 2-D tapered hydrofoil. An enthalpy conservation equation was solved along with the governing equation of the mixture. Although the temperature depression inside the cavity was reproduced, the temperature tendency was not matched the experimental data. A similar approach was then widely used in numerical simulation of thermodynamic effect on cavitation [7,8]. Anh et al. proposed a simplified thermodynamic effect model belong to the second approach, which was expressed in form of a mixture temperature equation [9,10]. In this model, the heat transfer due to evaporation/condensation was explicitly appeared and was adjusted to suit the homogeneous model. A CFD calculation for cavitating flow on a 2-D tapered hydrofoil in cryogenic liquids was validated. A better temperature profile was reproduced using this model compare with the existing numerical data by past researches for cryogenic liquids [6–8].

In this study, the cavitation in hot water, where the thermodynamic effect, phase change phenomena, and flow behavior are tightly coupled, is studied by combining the experiment and numerical simulation. The experiment is conducted in the high temperature and high-pressure water tunnel. The NACA0015 hydrofoil is selected as the cavitator. The temperature of the water is heated up to 90°C. The temperature difference between the cavity and freestream is measured using the high accuracy thermistor probe. The CFD simulation is then conducted and compared quantitatively with the experimental data. This work aims to clarify the applicability of our simplified thermodynamic model, which has been successfully applied for cryogenics liquids, for the prediction of

hot water cavitation. Moreover, the flow behaviors such as temperature effect and velocity effect are emphasized.

2. MEASUREMENTS

2.1. Experimental setup

The cavitation experiment in hot water was studied in high temperature and high-pressure water tunnels as on the left side of Fig. 1. In this tunnel, the pressure can rise to 0.5 MPa, and the temperature can heat up to 140°C using an electric heater with an accuracy of 0.1°C. The test section is a channel with 30 mm $\times$ 20 mm in cross-section and 330 mm in length. An observation window, made of glass, was installed to test the section to enable the visualization of cavitation appearance. The tank pressure was controlled using a compressor and vacuum pump; the flow rate was adjusted by controlling the pump rotation speed. The upstream and downstream pressures of the object were measured using a pressure transducer. In this study, the NACA0015 hydrofoil with a chord length of 40 mm and 20 mm span width, which is based on Yamaguchi's work [3], was used. The angle of attack was at 12 degrees. Two thermistor probes with high accuracy (Nikkiso-Thermo Co., Ltd.) were inserted to the mid-span of the channel to measure the freestream temperature T_0 (ThP1) and cavity temperature T_c (ThP2) as in the right

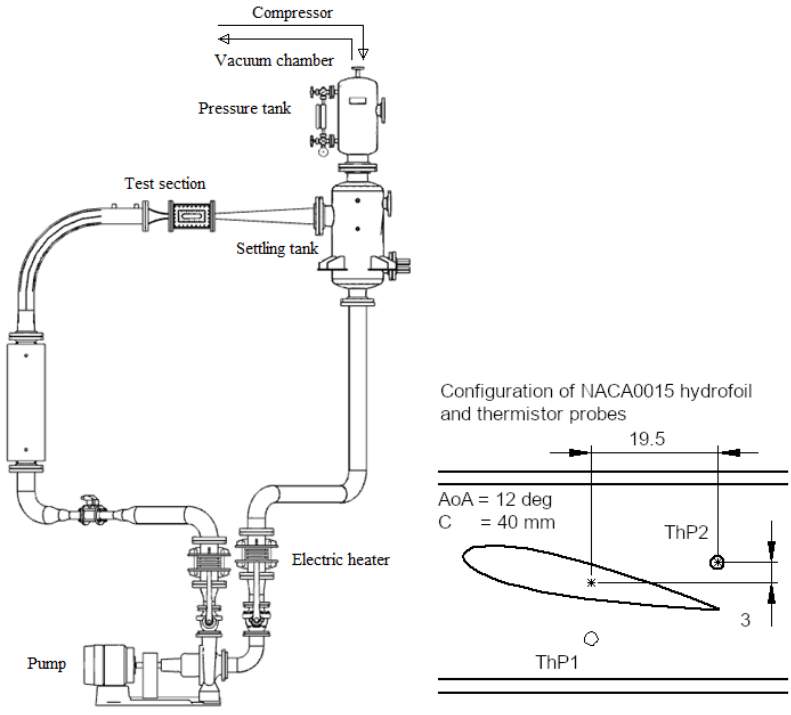

Fig. 1. Overview of (left) high temperature – high pressure water tunnel and (right) the configuration of NACA0015 hydrofoil with two thermistor probes (the dimension is in mm)

side of Fig. 1. These thermistor probes were calibrated using a TAKASAGO thermometer. The resistance of the thermistor probe was measured using a digital multimeter. The high-speed charged-coupled device (CCD) camera was used to visualize the cavity aspect with a frame rate of 100,000 fps. The water was degassed with measured dissolved oxygen (DO) about 30%.

The freestream temperature was heated from room temperature up to 90°C. The flow velocity was adjusted from 6 m/s to 8 m/s. The cavitation number σ was varied by controlling the tank pressure. Five different flow temperatures have been experimented in this study. The temperature data were recorded every 2 seconds, and the measurement temperature was averaged in 30 seconds of measurement. The actual freestream temperature measured was about 1°C around the designed temperature. The experiment conditions are shown in Table 1.

Table 1. Experimental conditions for NACA0015 hydrofoil in water

<table>
<tr><td colspan="4">AoA = 12 Deg.</td></tr>
<tr><td rowspan="2">U_0 (m/s)</td><td colspan="2">Temperature (°C)</td><td rowspan="2">Cavitation number, σ</td></tr>
<tr><td>Designed, T_0</td><td>Actual</td></tr>
<tr><td rowspan="5">8</td><td>25</td><td>Not measured</td><td rowspan="4">1.60</td></tr>
<tr><td>60</td><td rowspan="4">Around 1°C of T_0</td></tr>
<tr><td>70</td></tr>
<tr><td>80</td></tr>
<tr><td>90</td><td>Varied</td></tr>
<tr><td>7</td><td rowspan="2">90</td><td rowspan="2">1.60</td></tr>
<tr><td>6</td></tr>
</table>

2.2. Cavitation visualization and measurement of temperature depression

Fig. 2 shows the instantaneous image of the appearance of cavity with freestream temperature of (a) T_0 = 25°C, (b) T_0 = 60°C, and (c) T_0 = 90°C on the condition of σ = 1.6, U_0 = 8 m/s. Notably, the thermistor probes were not inserted in the experiment at T_0 = 25°C. The shedding cavitation was visualized at T_0 = 25°C. Higher temperature, the supercavitation occurred and the second thermistor probe (ThP2) was fully immersed inside the cavity. According to the visualization, the inverse thermodynamic effect was observed. Cavity became longer with the increase of freestream temperature. At high-temperature T_0 = 90°C, the stronger cavitation was visualized compare to T_0 = 60°C, in that the cavity length was over the observation window. Similar behavior was also reported in Cervone's experiment [4].

Fig. 3 shows the relation of measured temperature depression with freestream temperature on the condition of σ = 1.6, U_0 = 8 m/s. The freestream temperature was varied from 60°C to 90°C. The measured result was compared with the experimental data of

Yamaguchi [3]. The standard uncertainty was about 0.01°C. According to the results, the temperature depression became bigger when the freestream temperature increases. The measured temperature depression agreed with Yamaguchi's data up to 80°C. The temperature drop was measured at about 0.32°C at a freestream temperature of $T_0 \approx 90$°C. Although the cavitation appeared on the supporting pipe of ThP1. The appearance place was far away from the thermistor probe heat, the effect of cavitation on the measurement data is thus negligible.

Fig. 4 shows the measured temperature depression in the cavity regarding the cavitation number on the condition of $U_0 = 8$ m/s, $T_0 \approx 90$°C. The temperature drop inside the cavity increased when the cavitation number getting smaller. The supercavitation was visualized at cavitation number $\sigma \leq 1.6$. The non-cavitation and the developing cavitation were visualized at cavitation number $\sigma > 2$ in this study. Regarding the supercavitation region, the temperature depression increased rapidly as the cavitation number decreases. Since we could not further reduce the cavitation number $\sigma < 1.5$, the maximum temperature depression

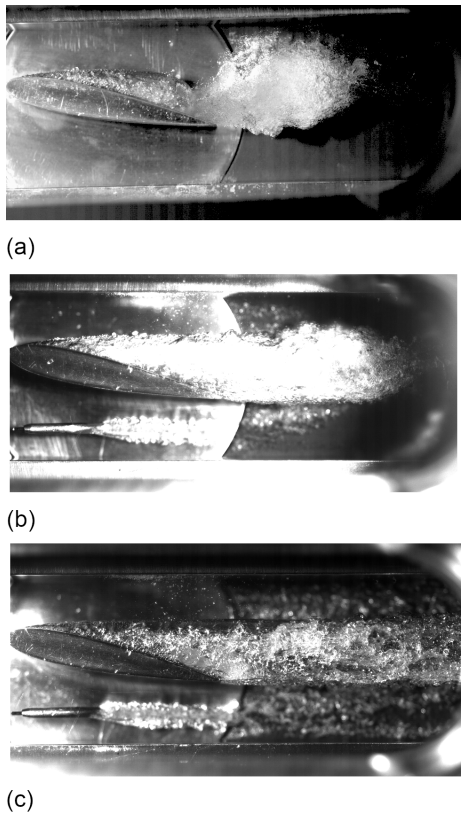

Fig. 2. The visualization of cavitation aspect at: (a) $T_0 = 25$°C, (b) $T_0 = 60$°C, and (b) $T_0 = 90$°C ($\sigma = 1.6$, $U_0 = 8$ m/s)

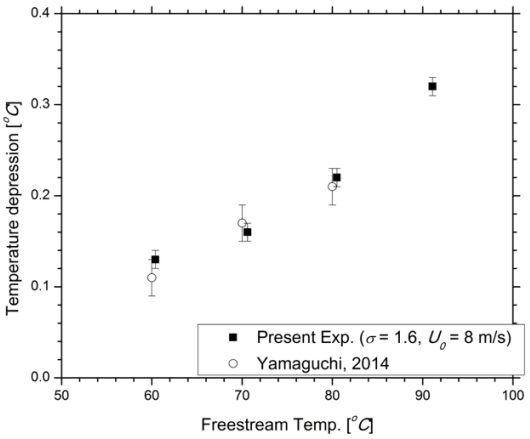

Fig. 3. Measurement of temperature depression regarding to different freestream temperature ($\sigma = 1.6$, $U_0 = 8$ m/s)

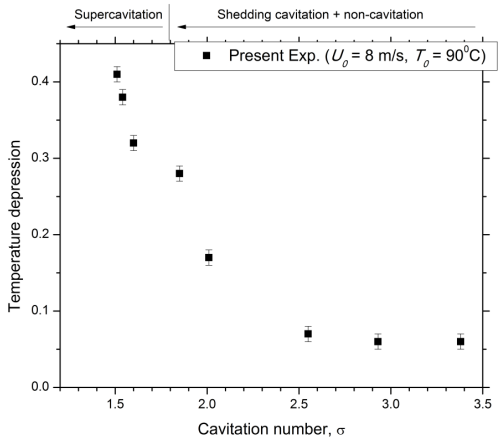

Fig. 4. The influence of cavitation number on the measurement of temperature depression ($U_0 = 8$ m/s, $T_0 \approx 90$°C)

was measured at about 0.41°C in this study. For $\sigma > 2$, where the cavity did not reach the second thermistor probe ThP2, the temperature difference between the two thermistor probes was relatively small. The difference in measured results may cause by the diffusion effect at two thermistor probes. For $1.6 < \sigma < 2$, the shedding cavitation, in which the ThP2 was covered by both vapor and pure water cyclically, occurred. Then, the temperature depression became bigger in comparison with the higher cavitation number. However, the measured temperature depression in this region was sensitive and therefore difficult to adjust the accuracy. The instantaneous image of cavitation aspect at two different cavitation numbers (a) σ = 1.85 – the shedding cavitation and (b) σ = 1.6 – the supercavitation are shown in Fig. 5.

Fig. 6 shows the dependence of the temperature depression regarding the freestream velocity on the flow condition of σ = 1.6, $T_0 \approx 90$°C. The nonlinear relationship of temperature depression and freestream velocity was observed. The temperature depression decreases with the increase of freestream velocity. At U_0 = 6 m/s, the temperature difference was measured about 0.39°C. The lower temperature depression was recorded at the freestream velocity U_0 = 7 m/s, and U_0 = 8 m/s.

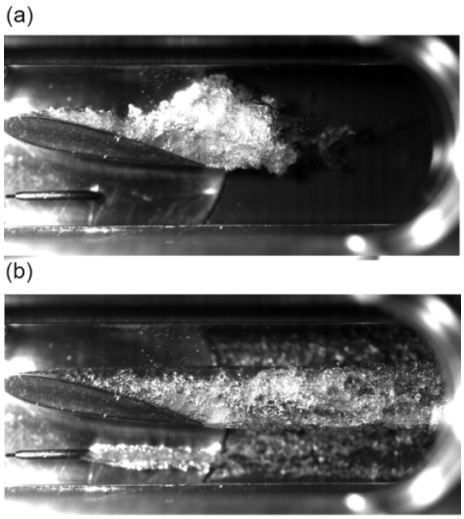

Fig. 5. Appearance of cavity in water (U_0 = 8 m/s, T_0 = 90°C): (a) σ = 1.85 – the shedding cavitation and (b) σ = 1.6 – the supercavitation

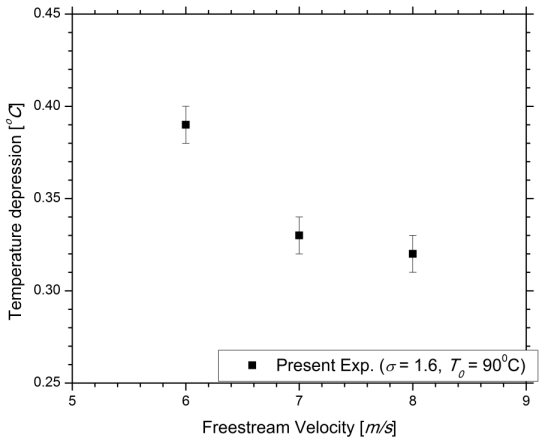

Fig. 6. Dependence of temperature depression regarding to freestream temperature (σ = 1.6, $T_0 \approx 90$°C)

3. SIMULATION

3.1. Numerical method

The cavitating flow was simulated using the homogeneous model approach. In that, the phases are assumed to share the same pressure, temperature, and velocity. The liquid phase is assumed to be a compressible fluid and the equation of state is derived from Tammann's equation [11]. The gas phase is assumed to be an ideal gas. Therefore,

the governing equations for the locally homogeneous compressible two-phase medium can be written in a simple form as for single-phase flow. In addition, a mass conservation equation for the gas phase is implemented that includes the phase change rate due to cavitation in the source term. The equation of state is reconstructed to close the systems [12, 13]. The standard $k - \omega$ turbulent model was used for accounting for the effect of turbulence on cavitation [14]. A cavitation model based on the Herz-Knudsen-Langumur equation [15] is used for modeling the mass transfer rate m when cavitation occurs/collapses. The influence of turbulence on the threshold vapor pressure $p_v(T)^*$ was calculated based on Singhal's suggestion [16]. As in the experiment, the temperature depression increase with the increase of water temperature. To account for this phenomenon, a simplified thermodynamic model, which has been validated for cryogenic liquids [10], is used. The detail of the systems governing equation can be referred to the work by Anh et al. [10].

3.2. Numerical scheme

The compressible unsteady cavitating flow was simulated by an in-house code based on the finite difference method (FDM). The explicit (Total Variation Diminishing) TVD Maccormack scheme [17,18], which is a predictor-corrector type scheme, was used. Backward and forward discretization was used in the predictor and corrector steps, respectively. In the numerical simulation of cavitating flow, the strong pressure wave is generated; hence, the second-order symmetric TVD scheme [18] was applied after the corrector step to ensure stability and monotonicity of the solution. The viscous terms were discretized by a second-order space-centered scheme. Hence, this scheme has second-order accuracy in time and space. The scalable wall function was used [19]. This numerical scheme was validated for cavitating flow in cryogenic liquids and water at room temperature [9].

3.3. Computational conditions

A C-type orthogonal boundary fitted grid (253 $\times$ 70) was made over the hydrofoil as in Fig. 7. In that, the inlet is located at three-chord length from the leading edge of hydrofoil; the outlet is located at five chord length from the trailing edge. At the inlet, a uniform velocity, temperature, void fraction, and turbulent quantities were specified. The

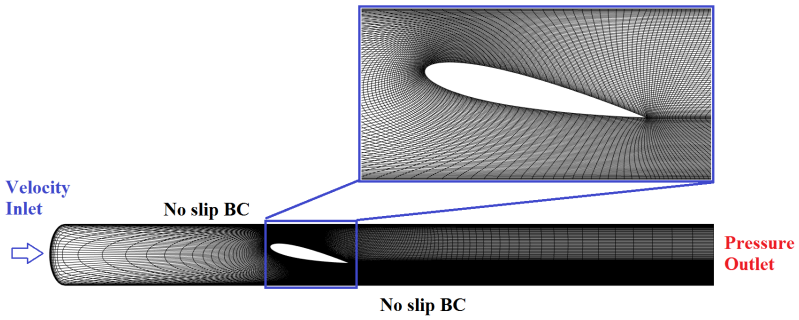

Fig. 7. Computational grid for NACA0015

pressure regarding the experimental cavitation number was set at a reference point in the inlet boundary. The static pressure was set at the outlet 7 boundaries. No slip condition was applied at the top/bottom wall and hydrofoil. The five runs of the experiment were selected in this study as in Table 2, and the numerical results were compared with the experimental data based on the visualized image and measured temperature depression.

Table 2. Calculation conditions for NACA0015 hydrofoil in hot water

AoA =12 deg.						
U_0 (m/s)	Runs	σ	Designed Temperature T_0 (°C)			
			25	60	70	90
8	Run0	1.60	×			
	Run1			×		
	Run2				×	
	Run3					×
6	Run4	1.60				×

3.4. Results and discussion

3.4.1. *Influence of freestream temperature*

Fig. 8 shows a comparison of the time-averaged temperature depression obtained by the numerical simulation and experimental data according to freestream temperature on supercavitation condition: run1 (σ = 1.60, U_0 = 8 m/s, T_0 = 60.6°C), run2 (σ = 1.60, U_0 = 8 m/s, T_0 = 70.7°C), and run3 (σ = 1.60, U_0 = 8 m/s, T_0 = 91°C). The quantitatively good agreement in temperature depression was reproduced in all runs. The tendency of temperature depression agreed with experimental data, in that the degree of temperature drop in simulation was increased with the increase of freestream temperature.

Fig. 9 shows the comparison of numerical result and experimental data in run1 (σ = 1.60, U_0 = 8 m/s, T_0 = 60.6°C) – (left) and run3 (σ = 1.60, U_0 = 8 m/s, T_0 = 91°C) – (right), respectively. In the figures, (a) is the instantaneous image of the cavity in the experiment, (b) is the instantaneous image of the cavity in numerical simulation, and (c) is temperature distribution. Although it is difficult to completely compare the cavity length because of the random bubble cloud at the rear of the cavity, the cavity aspect showed good agreement compare with the experiment in run1 (σ = 1.60, U_0 = 8 m/s, T_0 = 60.6°C). As freestream temperature shifts toward around T_0 = 90°C, the supercavitation became stronger with longer cavity length in both numerical and experiment. The minimum temperature appeared at the region behind the hydrofoil trailing edge, where the vapor void fraction is high.

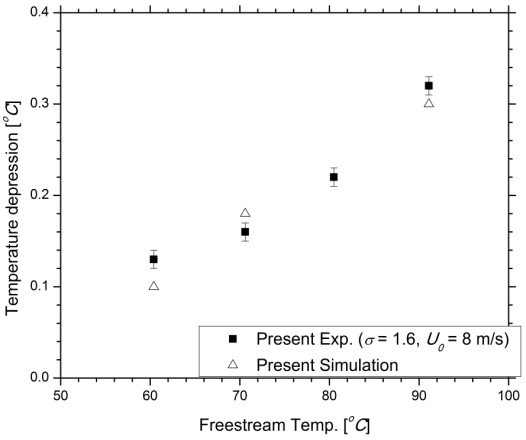

Fig. 8. Comparison of temperature depression between numerical simulation and experiment in run1 ($\sigma = 1.60$, $U_0 = 8$ m/s, $T_0 = 60.6$°C), run2 ($\sigma = 1.60$, $U_0 = 8$ m/s, $T_0 = 70.7$°C), and run3 ($\sigma = 1.60$, $U_0 = 8$ m/s, $T_0 = 91$°C)

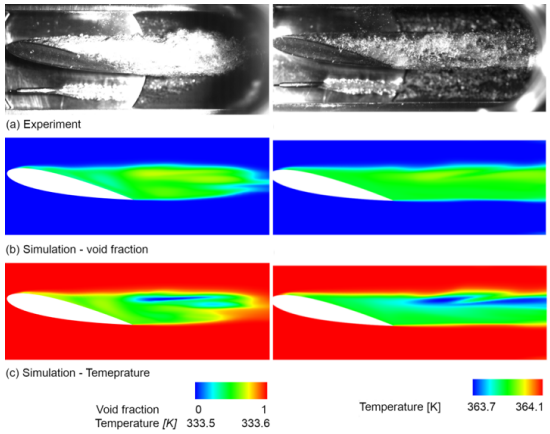

Fig. 9. Instantaneous distribution of cavity aspect in experiment (a), vapor void fraction in simulation (b), and temperature distribution (c) in run1 ($\sigma = 1.60$, $U_0 = 8$ m/s, $T_0 = 60.6$°C) – (left), and run3 ($\sigma = 1.60$, $U_0 = 8$ m/s, $T_0 = 91$°C) – (right)

3.4.2. *Influence of freestream velocity*

Fig. 10 illustrates the comparison of the temperature depression between the present numerical solution and the experiment data at $T_0 = 90$°C with different freestream velocities. The temperature depression inside the cavity is decreased when the velocity

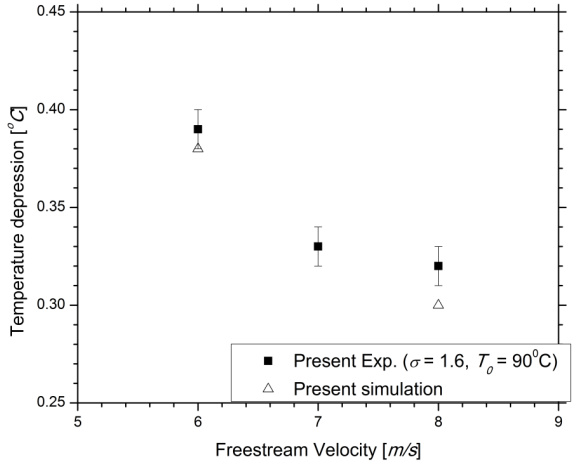

Fig. 10. Comparison of temperature depression between simulation and experiment in run3 ($\sigma = 1.60$, $U_0 = 8$ m/s, $T_0 = 91$°C), and run4 ($\sigma = 1.60$, $U_0 = 6$ m/s, $T_0 = 90.3$°C)

increase. The numerical results agreed with the measured data. Notably, previous studies showed that the temperature depression inside the cavity is proportional to the non-dimensional thermodynamic parameter Σ^* in Eq. (1) [20,21]. Table 3 depicts the Σ^* with respect to the freestream velocity. It is clear that the Σ^* becomes smaller as the velocity increases, the temperature depression is thus smaller. This behavior was consistent with the present simulation results.

$$\Sigma^* = \frac{\rho_v^2 L^2}{\rho_l^2 C_{pl} T_\infty \sqrt{a_l}} \sqrt{\frac{C}{U_\infty^3}}, \tag{1}$$

where ρ is the fluid density and c is the chock length of the hydrofoil. In addition, C_p, α_l, and L are the specific heat capacity, the thermal diffusivity, and the latent heat of the water. The subscripts v and l stand for the vapor and water phases, respectively.

Table 3. Non-dimensional thermodynamic parameter for water at a different flow velocity

$T_0 \approx 90°C$			
U_0 (m/s)	6	7	8
Σ^*	21.88	17.36	14.21

4. CONCLUSIONS

In this paper, cavitation in hot water was studied by combined experimental and numerical simulation approaches. The experiment was performed in the high temperature and high-pressure water tunnel with NACA0015 as cavitator. Different flow conditions such as temperature, velocity, and cavitation number, were conducted. The temperature depression inside the cavity was measured using the high-accuracy thermistor probe. The numerical solution was conducted based on experimental data by coupling a simplified thermodynamic model and governing equation.

As in the experiment, the temperature depression in the cavity was increased proportionally with the increase of freestream temperature. The maximum temperature depression of about 0.41°C was measured in water at 90°C in this experiment. However, the inverse thermodynamic effect was observed, although the temperature drop was observed inside the cavity. The reason is still unclear.

The cavitation phenomena in hot water cavitation were successfully reproduced using a simplified thermodynamic model. The temperature drop and cavity volume were well predicted. The temperature depression tendency in the cavity agreed with experimental data under different flow conditions with a relatively small difference. Finally, it concludes that the present simplified thermodynamic model is applicable for simulating the thermodynamic effect on cavitation in different liquids using the homogeneous model.

ACKNOWLEDGMENTS

This research is funded by Vietnam National Foundation for Science and Technology Development (NAFOSTED) under grant number 107.03-2020.22.

REFERENCES

[1] M. Petkovšek and M. Dular. IR measurements of the thermodynamic effects in cavitating flow. *International Journal of Heat and Fluid Flow*, **44**, (2013), pp. 756–763. https://doi.org/10.1016/j.ijheatfluidflow.2013.10.005.

[2] M. Petkovšek and M. Dular. Observing the thermodynamic effects in cavitating flow by IR thermography. *Experimental Thermal and Fluid Science*, **88**, (2017), pp. 450–460. https://doi.org/10.1016/j.expthermflusci.2017.07.001.

[3] Y. Yamaguchi and Y. Iga. Thermodynamic effect on cavitation in high temperature water. In *Fluids Engineering Division Summer Meeting*, American Society of Mechanical Engineers, (2014).

[4] A. Cervone, C. Bramanti, E. Rapposelli, and L. d'Agostino. Thermal Cavitation Experiments on a NACA 0015 Hydrofoil. *Journal of Fluids Engineering*, **128**, (2005), pp. 326–331. https://doi.org/10.1115/1.2169808.

[5] S.-I. Tsuda, N. Tani, and N. Yamanishi. Development and Validation of a Reduced Critical Radius Model for Cryogenic Cavitation. *Journal of Fluids Engineering*, **134**, (2012). https://doi.org/10.1115/1.4006469.

[6] A. Hosangadi and V. Ahuja. Numerical Study of Cavitation in Cryogenic Fluids. *Journal of Fluids Engineering*, **127**, (2005), pp. 267–281. https://doi.org/10.1115/1.1883238.

[7] Y. Utturkar, J. Wu, G. Wang, and W. Shyy. Recent progress in modeling of cryogenic cavitation for liquid rocket propulsion. *Progress in Aerospace Sciences*, **41**, (2005), pp. 558–608. https://doi.org/10.1016/j.paerosci.2005.10.002.

[8] C. C. Tseng and W. Shyy. Turbulence Modeling for Isothermal and Cryogenic Cavitation. In *47th AIAA Aerospace Sciences Meeting including The New Horizons Forum and Aerospace Exposition*, American Institute of Aeronautics and Astronautics, (2009), https://doi.org/10.2514/6.2009-1215.

[9] A. D. Le, J. Okajima, and Y. Iga. Modification of Energy Equation for Homogeneous Cavitation Simulation With Thermodynamic Effect. *Journal of Fluids Engineering*, **141**, (2019). https://doi.org/10.1115/1.4042257.

[10] A. D. Le, J. Okajima, and Y. Iga. Numerical simulation study of cavitation in liquefied hydrogen. *Cryogenics*, **101**, (2019), pp. 29–35. https://doi.org/10.1016/j.cryogenics.2019.04.010.

[11] H.-T. Chen and R. Collins. Shock wave propagation past an ocean surface. *Journal of Computational Physics*, **7**, (1971), pp. 89–101. https://doi.org/10.1016/0021-9991(71)90051-9.

[12] Y. Iga, M. Nohmi, A. Goto, B. R. Shin, and T. Ikohagi. Numerical Study of Sheet Cavitation Breakoff Phenomenon on a Cascade Hydrofoil. *Journal of Fluids Engineering*, **125**, (2003), pp. 643–651. https://doi.org/10.1115/1.1596239.

[13] Y. Iga, M. Nohml, A. Goto, and T. Ikohagi. Numerical Analysis of Cavitation Instabilities Arising in the Three-Blade Cascade. *Journal of Fluids Engineering*, **126**, (2004), pp. 419–429. https://doi.org/10.1115/1.1760539.

[14] D. C. Wilcox. *Turbulence modeling for CFD*. DCW industries La Canada, CA, (1994).

[15] N. Ochiai, Y. Iga, M. Nohmi, and T. Ikohagi. Numerical Prediction of Cavitation Erosion Intensity in Cavitating Flows around a Clark Y 11.7% Hydrofoil. *Journal of Fluid Science and Technology*, **5**, (3), (2010), pp. 416–431. https://doi.org/10.1299/jfst.5.416.

[16] A. K. Singhal, M. M. Athavale, H. Li, and Y. Jiang. Mathematical Basis and Validation of the Full Cavitation Model. *Journal of Fluids Engineering*, **124**, (2002), pp. 617–624. https://doi.org/10.1115/1.1486223.

[17] R. Maccormack. The effect of viscosity in hypervelocity impact cratering. In *4th Aerodynamic Testing Conference*, American Institute of Aeronautics and Astronautics, (1969). https://doi.org/10.2514/6.1969-354.

[18] H. C. Yee. *Upwind and Symmetric Shock - Capturing Schemes*. NASA Technical Memorandum 89464, (1987).

[19] F. Menter and T. Esch. Elements of industrial heat transfer predictions. In *16th Brazilian Congress of Mechanical Engineering (COBEM)*, Uberlandia, Brazil, (2001).

[20] C. Brennen. The Dynamic Behavior and Compliance of a Stream of Cavitating Bubbles. *Journal of Fluids Engineering*, **95**, (1973), pp. 533–541. https://doi.org/10.1115/1.3447067.

[21] S. Watanabe, T. Hidaka, H. Horiguchi, A. Furukawa, and Y. Tsujimoto. Steady Analysis of the Thermodynamic Effect of Partial Cavitation Using the Singularity Method. *Journal of Fluids Engineering*, **129**, (2006), pp. 121–127. https://doi.org/10.1115/1.2409333.